RSC Advances

PAPER

View Article Online
View Journal | View Issue

Cite this: *RSC Adv.*, 2020, **10**, 34953

A N-doped porous carbon derived from deep eutectic solvent for adsorption of organic contaminants from aqueous or oil solution†

Chunyan Xiong, Fuchuan Liu, Jiajun Gao* and Xingmao Jiang*

Received 22nd May 2020
Accepted 6th September 2020

DOI: 10.1039/d0ra04542j

rsc.li/rsc-advances

Porous N-doped carbon material (NCM) derived from deep eutectic solvent (DES) is successfully prepared. The preparation of NCM depends mainly on heating treatment and does not demand activation and filtration. The heating process contains three steps: (1) forming a DES that consists of glucose and urea at 100 °C; (2) preparing dried precursors by microwave; (3) and carbonizing the precursor. After heating, the resulting NCM can be obtained. The as-prepared NCM exhibits high specific surface area, rich micropores and strong Lewis basicity. Accordingly, NCMs show good adsorption performance for 4-nitrophenol or methylene blue in aqueous solution and thiophenic sulfurs in the oil phase. Apparently, NCM derived from DES not only possesses a simple preparation process, but also can remove a wide spectrum of organic pollutants. Therefore, the NCM prepared here may be promising for practical application.

Introduction

Adsorption has been proven to be an effective technique for the removal of organic contaminants from aqueous or oil solution due to its simple operation and applicability for a wide range of contaminants. In addition, the saturated adsorbents could be easily regenerated or disposed of with low risk for the environment.[1,2] Because of the large specific area, carbon-based materials (CMs) are widely used adsorbents for removing phenols, dyes, or other contaminants from aqueous solutions.[3–7] Besides, it also can desulfurize fuel oils. However, pure carbon is hydrophobic. This leads to the poor dispersion in water and offsets the superior performance of the high surface area.[8] And its lack of active functional groups will also cause bad affinity with the organic species.[9] Hence, chemical modification that strengthens the polarity and improves surface groups is necessary. For their modification, carbons are usually activated by acidic and basic solutions, such as HNO_3, H_2SO_4, KOH, and NaOH. The activation agent inevitably produces waste acids or bases that were difficult in treatment and further increases the cost.[10] In addition, the excessive modification not only corrodes the equipment but also may break down the porous structure of CMs.[11] Therefore, controlling the modification is not a simple matter.

In recent years, N-doped carbon materials (NCMs) have been highly effective adsorbents.[12] The N-element could modulate the hydrophilicity of carbon materials and enhance the Lewis basicity thereof. They show excellent adsorption performance and so attract a lot of attentions.[10,11] Nevertheless, NCMs need to be prepared *via* various hard or soft templates and activation agent (such as NaOH) that have to be removed by solvent washing. So, their preparation undergoes the high cost. What's worse, the filtration operation, which is unfavorable in industry, seems inevitable for the preparation process. The disadvantages undoubtedly limit the industrial production of NCMs.

In this contribution, a NCM with high specific surface area was successfully prepared *via* deep eutectic solvent (DES) composed of glucose and urea. The preparation showed the following advantages. First, the whole process only depends on heating and did not involve the activation and the filtration. Second, DES was a homogenous liquid phase, and accordingly its composition can be easily controlled by mole ratio of glucose and urea. Third, the process did not produce the wastewater hard to be treated. Moreover, the prepared NCM can effectively eliminate the organic pollutants from aqueous or oil solution. Therefore, deriving NCM from DES may be a promising method for the preparation of adsorbent with high performance.

Experimental section

Synthesis

All the reagents used in the current work were purchased from commercial suppliers and used without further purification.

Hubei Provincial Research Centre of Engineering & Technology for New Energy Materials, Key Laboratory for Green Chemical Process of Ministry of Education, School of Chemical Engineering & Pharmacy, Wuhan Institute of Technology, Wuhan 430205, China. E-mail: gaojiajun@wit.edu.cn; jxm@wit.edu.cn; Tel: +86 2787194980

† Electronic supplementary information (ESI) available: Table S1: title, porous structure parameters of NCMs, Table S2: XPS data-envelope of O1s for NCM-2, Table S3: XPS data-envelope of N1s for NCM-2. See DOI: 10.1039/d0ra04542j

0.1 mol glucose (Aladdin, 99%) was mixed with urea (Aladdin, 99%) of 0.3 mol, 0.5 mol, 0.6 mol, and 0.7 mol, separately. As shown in Fig. 1, clear and transparent viscose liquids were formed by heating the mixtures in the beakers using oil bath at 100 °C, and then they were mixed by magnetic stirring for 2 h. After that, the above DESs formed by glucose and urea were heated and dried by microwave with power of 900 W for 5 min. Black foam-like products were obtained, and they were then carbonized in a nitrogen atmosphere to obtain the porous NCMs. The detail carbonization condition was as follows: (1) heating from room temperature to 350 °C at the rate of 2°C min^{-1}; (2) 350 °C lasting for 4 h; (3) heating to 900 °C at the rate of 2°C min^{-1}; (4) 900 °C lasting for 10 h. The materials synthesized with the mole ratio for glucose and urea of 1 : 3, 1 : 5, 1 : 6, and 1 : 7 were denoted as NCM-1, NCM-2, NCM-3, and NCM-4 in short for the following part.

Characterization

The specific surface areas and the pore volumes were analyzed by N_2 adsorption and desorption isotherms obtained at −196 °C on a Quantachrome Autosorb iQ analyzer. The specific surface areas of the samples were calculated *via* Brunauer–Emmett–Teller (BET) method at the relative pressure range of 0.05–0.3. So, they can be abbreviated as S_{BET}. The total pore volume (V_{total}) was calculated from the adsorption data using the program AutoSob IQ. The *t*-plot method was used to calculate the specific surface areas for micropore (S_{mic}) and mesopore volume (S_{meso}). The density functional theory method was used to evaluate the pore size distributions. To characterize the functional groups of materials, we employed FT-IR (Tensor II). The morphologies of the obtained materials were observed on the scanning electron microscopy (SEM, Smart LabSE) and the transmission electron microscopy (TEM, JEM 1010). X-ray photoelectron spectroscopy (XPS) was carried out with Thermo ESCALAB 250 XI using monochromatic Al Kα radiation.

Adsorption test

The adsorption experiment was conducted in a batch vessel under room temperature and ambient pressure. For adsorption kinetics, 10.0000 g of solution was mixed with 0.0100 g NCM under vigorous magnetic stirring. A portion of solutions were withdrawn at different time interval; for adsorption isotherm, the sample was stirred for 4 h to ensure the adsorption equilibrium. 10.0000 g of solution was mixed with a certain amount of NCM (*e.g.*, 0.1000 g or 0.0100 g) under vigorous magnetic stirring. The solution contained the aqueous or the oil. The aqueous solution consisted of water and an organic pollutant like 4-nitrophenol (4-NP) or methylene blue (MB). The oil was composed of *n*-octane and a thiophenic sulfur such as dibenzothiophene (DBT) or 4,6-dimethyldibenzothiophene (4,6-DMDBT). The contents of solutes were all set as 1000 μg g^{-1}. After the adsorption, the residual contents of solutes were detected by high performance liquid chromatography (Shimadzu, LC2030) or sulfur–nitrogen analyzer (KY-3000SN, Keyuan Electronic Instrument Ltd.).

The adsorption kinetics was also studied by pseudo-second-order models:

$$\frac{t}{Q_t} = \frac{1}{KQ_e^2} + \frac{t}{Q_e} \quad (1)$$

where t and Q_t refer to adsorption time and adsorbance, respectively. Parameters Q_e and K were denoted as adsorbance at equilibrium and the adsorption rate constant, respectively.[13–15]

The equilibrium concentration of 4-NP and MB, C_e (mg L^{-1}), was determined and the equilibrium capacity, Q_e (mg g^{-1}), was calculated by the following:

$$Q_e = \frac{(C_0 - C_e)V}{W} \quad (2)$$

where C_0 is the initial concentration (mg L^{-1}), and V is the volume of the solution (L), and W is the mass of the NCM (g).

The adsorption isotherm data of NCM to 4-NP and MB were correlated by the Langmuir model and the Freundlich models. The Langmuir models is as follows:[16]

$$Q_e = \frac{Q_m K_L C_e}{1 + K_L C_e} \quad (3)$$

where Q_m and K_L are the saturated absorbance (mg g^{-1}) and the Langmuir constant (L mg^{-1}). The Freundlich model is shown as the following:[17]

$$Q_e = K_F C_e^{\frac{1}{n}} \quad (4)$$

where K_F and $1/n$ refer to the indicator of adsorption capacity and adsorption intensity.

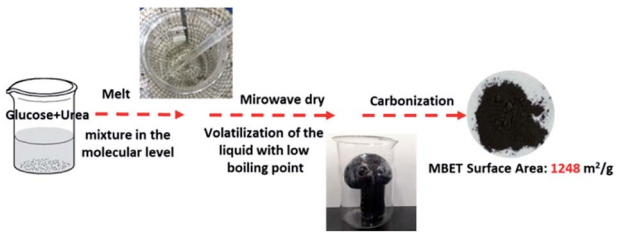

Fig. 1 Preparation process for NCMs.

Results and discussion

As tested previously, the viscous liquid can be formed at 100 °C when glucose and urea were mixed with each other. The phenomenon suggested the formation of DES because melting points of glucose and urea are both above 130 °C. After heating treatment (microwave and carbonization), the black powder (NCMs) can be obtained. The drying and heating process including a series of reactions such as the water loss in the first step, followed by a series of endothermic reactions such as deamination, dehydration of ketosamines, deamination of isomerized α-dicarbonyl and accumulation of hydroxymethylfurancarboxaldehyde.[18] The results of porous structure parameters for the as-prepared NCMs are presented in Fig. 2a. The contribution of mesopore to NCMs is very limited, as evidenced by the fact that S_{mic} is much larger than S_{meso}. In addition,

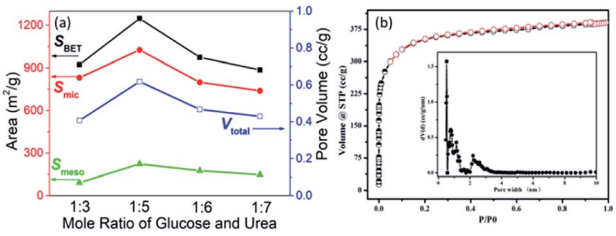

Fig. 2 (a) Comparison of porous structure parameter among NCMs. (b) Nitrogen adsorption/desorption isotherm and pore size distribution of NCM-2.

NCM-2 shows the highest specific surface area of 1248 m^2 g^{-1} and the highest pore volumes of 0.618 cm^3 g^{-1}. The detailed data of the porous structure can be seen in Table S1.† The excellent porous structure of NCM-2 may be caused by the proper molar ratio of glucose and urea. As is well known, DES consists of H-bonding donor (HBD) and H-bonding acceptor (HBA). The molar ratio of 1 : 5 means that the number of –OH (HBD) is equal to that of C=O (HBA). At this ratio, DES composed of glucose and urea possesses homogeneity. Assumedly, the homogenous distribution of HBD and HBA will be beneficial to the pore formation with the heating and carbonization. Further, NCM-2 can be identified as type I isotherm with a typical microporous nature, as shown in Fig. 2b. The pore size distribution indicates that rich microscopes and small mesopores exist, and that the pore size range from 1 nm to 4 nm.

The morphology and microstructure of NCM-2 were further presented by the images of SEM and TEM. In Fig. 3a and b, NCM-2 shows membrane-like structure. The surface is smooth, but the inner structure is coarse. This is probably due to its porous inner structure. Fig. 3c and d shows the TEM images of NCM-2. The large number of pores may bring in high SBET and large V_{total}.

The chemical composition of NCM-2 was further characterized by XPS. As shown in Fig. 4a, the survey spectrum reveals the presence of C, N and O and the N-content amounts to 4.6 at% from the spectra collected. High resolution XPS was used to investigate the structure. The asymmetric high resolution C1s peaks shown in Fig. 4b has a little increased tendency. This indicates that a large portion of C atoms connected with N and O atoms. The high resolution of O1s spectrum indicates that the O atoms exist mainly in the form of C=O, R–OH, C–O–C and oxygen in bridge. The detailed quantitative data are shown in Table S2.† The high resolution N1s is used to probe the nature of N functionalities in NCM-2. Peak deconvolution is shown in Fig. 4d. The resolved N1s spectra shows four different peaks, revealing the presence of pyridinic N1 (398.2 ± 0.2 eV), pyrrolic N2 (399.9 ± 0.2 eV), quaternary or graphite N3 (400.9 ± 0.2 eV), and pyridine N-oxide N4 (401.8 ± 0.2 eV).[19] The quantitative results of relative percentage are calculated from the ratio area N1si/∑area N, which could be seen in Table S3.† On the basis of the XPS results, the majority of N atoms are associated with the formation of surface as pyrrolic and pyridinic nitrogens, and that the other N atoms are incorporated into the skeleton of the carbon as a member. It can be concluded that NCM-2 shows strong Lewis basicity due to the presence of those O- and N-containing groups.

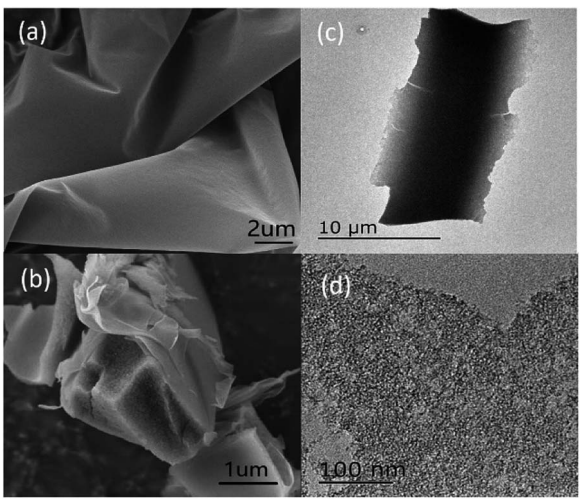

Fig. 3 (a and b) SEM images and (c and b) TEM images of NCM-2.

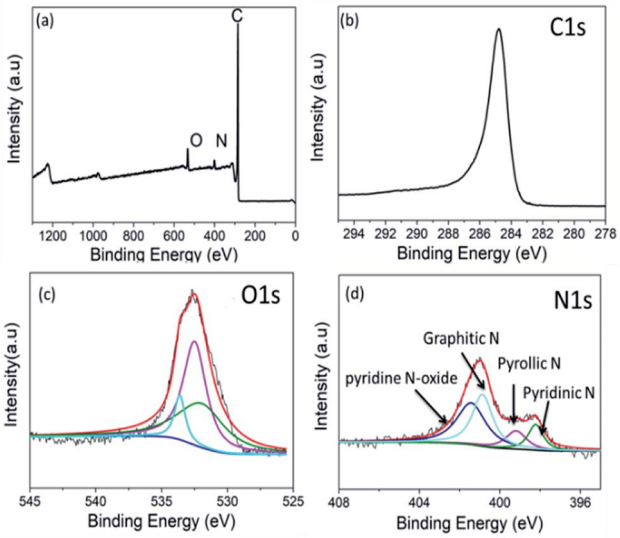

Fig. 4 (a) XPS survey spectrum of NCM-2, and (b–d) corresponding high resolution of C1s, N1s and O1s.

The surface chemistry of NCM-2 was also described by FT-IR spectrum. The results are shown in Fig. 5. The peak corresponding to the stretching vibration of O–H groups was found at 3435 cm^{-1},[20] while the small peak at 2920 cm^{-1} can be assigned to the stretching vibration of the –CH group,[21] stretching vibration of the –C=C bond was found at 1130 cm^{-1} (ref. 22) and the peak corresponding to the stretching vibration of C–O was located 1580 cm^{-1}.[23] The results are in consistence with the Raman results.

As stated previously, NCM-2 prepared in this work had the porous structure and the strong Lewis basicity. So, it may show good adsorption performance for the organic pollutants. In Fig. 6, 4-NP reached adsorption equilibrium very quickly; in

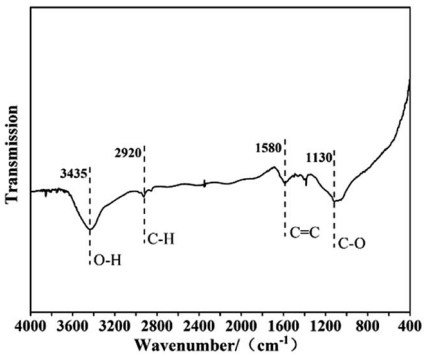

Fig. 5 FT-IR spectrum of NCM-2.

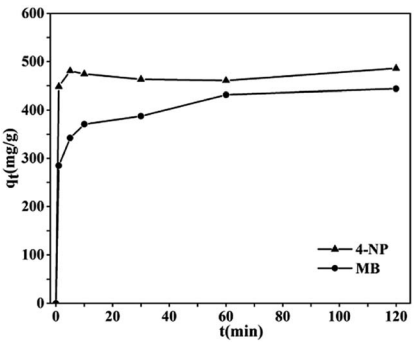

Fig. 6 Kinetic curves of adsorption of 4-NP and MB on NCM-2.

contrast, the MB samples have a relatively fast adsorption rate in the initial 15 minutes and followed by a slowly raised plateau. To further elucidate the controlling mechanism of 4-NP and MB adsorption over NCM-2, pseudo second-order was employed to simulate the kinetic parameters, as given in the ESI Table S4.† The correlation coefficients of the models are very high, and the results strongly suggested that the adsorption of both 4-NP and MB on NCM-2 is appropriately represented by a pseudo second-order rate process, the adsorption capacity and the adsorption rate of 4-NP is higher that of MB over the NCM-2. The low value at magnificent of 10^{-3} for the adsorption of 4-NP and MB over NCM-2 is comparable to the former investigations about chemical adsorption,[24] which could suggest the 4-NP and MB are more likely to be chemically absorbed.

The equilibrium isotherm describes how the adsorbent interact with the adsorbate. The adsorption isothermals were investigated and the results are shown in Fig. 7. The adsorption capacity of 4-NP on NCM-2 is lower than that of MB at low C_e, but the adsorption capacity of 4-NP on NCM-2 is higher than that of MB at high C_e. The adsorption isotherms are further fitted using two common models, the Langmuir and Freundlich. The fitting parameters are shown in Table S5.† According to the values of R^2, the Langmuir model is more suitable for the both the 4-NP and MB, which indicate the adsorption of 4-NP and MB is more tend to ascribe to homogenous adsorption. Combined with the results of adsorption kinetics, it could

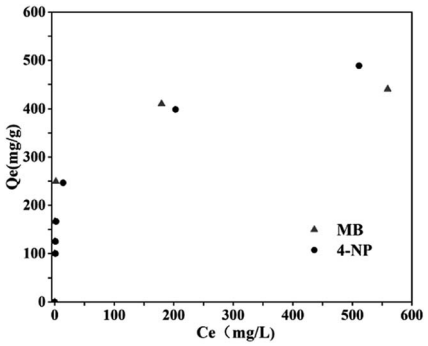

Fig. 7 Equilibrium isotherms of NCM-2 to MB and 4-NP.

conclude that the adsorption of 4-NP and MB is tend to ascribe to homogeneous chemical adsorption.

As shown in Fig. 8, NCM-2 can completely remove 4-NP or MB from the corresponding aqueous solution within only one minute. This implied that the adsorption of NCM-2 to the organic pollutants was very fast. The phenomenon is in consistent with the kinetic adsorption results. Apparently, NCM-2 showed much better affinity with 4-NP. This further suggested that, due to the strong Lewis basicity, NCM-2 had better affinity with the acidic pollutant.

In addition to the aqueous solution, the oil solution was also investigated. As described previously, NCM-2 was used to adsorb thiophenic sulfur (DBT or 4,6-DMDBT) from the model oil. The capacity was tested by the method described for 4-NP and MB. The S-capacity for DBT or 4,6-DMDBT can amount to 30.1 mg S g^{-1} (0.939 mmol g^{-1}) and 28.3 mg S g^{-1} (0.883 mmol g^{-1}), respectively. The results indicated that NCM-2 was not only effective for the pollutants in the aqueous solution, but also available for those in the oil phase. Therefore, NCM derived from DES shows good adsorption performance for a wide spectrum of organic pollutants.

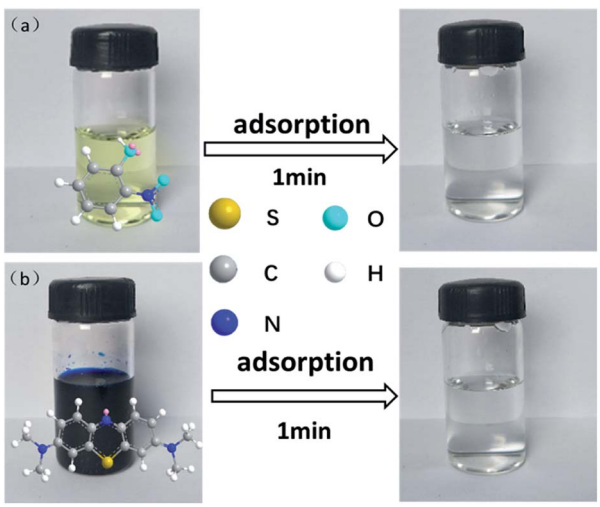

Fig. 8 Appearance of solution before and after adsorption by NCM-2. (Condition: $m_{NCM-2} = 0.1000$ g; $m_{solution} = 10.0000$ g; C4-NP or MB = 1000 μg g^{-1}; $T = 30$ °C).

Conclusion

NCM with high specific surface area, rich micropores and strong Lewis basicity was successfully prepared *via* DES composed of glucose and urea. The preparation process involved neither the activation nor the filtration operations. Moreover, the prepared NCM can effectively eliminate the organic pollutants from aqueous or oil solution. Therefore, deriving NCM from DES may be a promising method for the preparation of adsorbent with high performance.

Author contributions

Conceptualization, Chunyan Xiong and Fuchuan Liu; Fuchuan Liu; investigation, Chunyan Xiong, Jiajun Gao; data curation, Chunyan Xiong; writing—original draft preparation, Chunyan Xiong, Jiajun Gao; writing—review and editing, Xingmao Jiang.; supervision, authorship must be limited to those who have contributed substantially to the work reported.

Conflicts of interest

The authors declare no conflict of interest.

Acknowledgements

The research is supported by the National Natural Foundation of China (51702239, 21878237, and U1463210). The authors also acknowledge funding through project 17QD60 from Wuhan Institute of Technology and the funding through project X19D003 from Huazhong University of Science and Technology.

References

1 M. R. Samarghandi, T. J. Al-Musawi, A. Mohseni-Bandpi and M. Zarrabi, Adsorption of cephalexin from aqueous solution using natural zeolite and zeolite coated with manganese oxide nanoparticles, *J. Mol. Liq.*, 2015, **211**, 431–441.

2 M. A. Chayid and M. J. Ahmed, Amoxicillin adsorption on microwave prepared activated carbon from Arundo donax Linn: isotherms, kinetics, and thermodynamics studies, *J. Environ. Chem. Eng.*, 2015, **3**, 1592–1601.

3 *Kirk-Othmer Encyclopedia of Chemical Technology*, ed. J. I. Kroschwitz and M. Howe-Grant, John Wiley & Sons, New York, 1991, p. 1015.

4 *Ullmann's Encyclopedia of Industrial Chemistry*, ed. W. Gerhartz, Y. S. Yamamoto, F. T. Campbell, R. Pfefferkorn and J. F. Rounsaville, VCH Publishers, New York, 1985, p. 124.

5 E. D. Dimotakis, M. P. Cal, J. Economy, M. J. Rood and S. M. Larson, Chemically Treated Activated Carbon Cloths for Removal of Volatile Organic Carbons from Gas Streams: Evidence for Enhanced Physical Adsorption, *Environ. Sci. Technol.*, 1995, **29**, 1876.

6 W. E. Marshall and M. M. Johns, Agricultural By-Products as Metal Adsorbents: Sorption Properties and Resistance to Mechanical Abrasion, *J. Chem. Technol. Biotechnol.*, 1996, **66**, 192.

7 C. A. Toles, W. E. Marshall and M. M. Johns, Granular Activated Carbons from Nutshells for the Uptake of Metals and Organic Compounds, *Carbon*, 1997, **35**, 1407.

8 M. S. Mauter and M. Elimelech, Environmental applications of carbon-based nanomaterials, *Environ. Sci. Technol.*, 2008, **42**, 5843–5859.

9 Z. Q. Xua, Q. Q. Yang, J. Y. Lan, J. Q. Zhang, W. Peng, J. C. Jin, F. L. Jiang and Y. Liu, Interactions between carbon nanodots with human serum albumin and γ-globulins: The effects on the transportation function, *J. Hazard. Mater.*, 2016, **301**, 242–249.

10 R. Torregrosa-Macia, J. M. Martin-Martinez and M. C. Millelmeuer-Hazeleger, Porous Texture of Activated Carbons Modified with Carbohydrates, *Carbon*, 1997, **35**, 447.

11 C. Yu, X. Fan, L. Yu, *et al.*, Adsorptive Removal of Thiophenic Compounds from Oils by Activated Carbon Modified with Concentrated Nitric Acid, *Energy Fuels*, 2013, **27**, 1499–1505.

12 Y. Chong, K. Liu, Y. Liu, *et al.*, Highly efficient removal of bulky tannic acid by millimeter-sized nitrogen-doped mesoporous carbon beads, *AIChE J.*, 2017, **63**, 3016–3025.

13 R. I. Yousef, B. El-Eswed and A. a. H. Al-Muhtaseb, Adsorption characteristics of natural zeolites as solid adsorbents for phenol removal from aqueous solutions: kinetics, mechanism, and thermodynamics studies, *Chem. Eng. J.*, 2011, **171**(3), 1143–1149.

14 J. J. Gao, Y. F. Dai, W. Y. Ma, H. H. Xu and C. X. Li, Efficient separation of phenol from oil by acid–base complexing adsorption, *Chem. Eng. J.*, 2015, **281**, 749–758.

15 Y. Xiao, J. Azaiez and J. M. Hill, Erroneous Application of Pseudo-Second-Order Adsorption Kinetics Model Ignored Assumptions and Spurious Correlations, *Ind. Eng. Chem. Res.*, 2018, **57**, 2705–2709.

16 F. An, R. Du, X. Wang, M. Wan, X. Dai and J. Gao, Adsorption of phenolic compounds from aqueous solution using salicylic acid type adsorbent, *J. Hazard. Mater.*, 2012, **201–202**, 74–81.

17 O. Hamdaoui and E. Naffrechoux, Modeling of adsorption isotherms of phenol and chlorophenols onto granular activated carbon. Part I. Two-parameter models and equations allowing determination of thermodynamic parameters, *J. Hazard. Mater.*, 2007, **147**, 381–394.

18 X. B. Wang, Y. J. Zhang, C. Y. Zhi, X. Wang, D. M. Tang, Y. B. Xu, Q. H. Weng, X. F. Jiang, M. Mitome, D. Golberg and Y. Bando, *Nat. Commun.*, 2013, **4**, 2905.

19 P. Burg, *et al.*, The characterization of nitrogen-enriched activated carbons by IR, XPS and LSER methods, *Carbon*, 2002, **40**, 1521–1531.

20 H. Cai, X. An, J. Cui, J. Li, S. Wen, K. Li, M. Shen, L. Zheng, G. Zhang and X. Shi, Facile Hydrothermal Synthesis and Surface Functionalization of Polyethyleneimine-Coated Iron Oxide Nanoparticles for Biomedical Applications, *ACS Appl. Mater. Interfaces*, 2013, **5**, 1722–1731.

21 A. Nasrullah, H. Khan, A. S. Khan, Z. Man, N. Muhammad, M. I. Khan and N. M. Abd El-Salam, Potential biosorbent

derived from Calligonum polygonoides for removal of methylene blue dye from aqueous solution, *Sci. World J.*, 2015, **2015**, 1–11.

22 J. C. Durán-Valle, M. Gómez-Corzo, J. Pastor-Villegas and V. Gómez-Serrano, Study of cherry stones as raw material in preparation of carbonaceous adsorbents, *J. Anal. Appl. Pyrolysis*, 2004, **73**, 59–67.

23 M. Xie, J. Tang, G. Fang, M. Zhang, L. Kong, F. Zhu, L. Ma, D. Zhou and J. Zhan, Biomass Schiff base polymer-derived N-doped porous carbon embedded with CoO nanodots for adsorption and catalytic degradation of chlorophenol by peroxymonosulfate, *J. Hazard. Mater.*, 2020, **384**, 121345.

24 K. Zhang, Q. Wang, Y. Zhou, J. Gao, C. Li and X. Jiang, A low-cost crosslinked polystyrene derived from environmental wastes for adsorption of phenolic compounds from aqueous solution, *J. Mol. Liq.*, 2020, **314**, 1–8.